

Portland State University

**PDXScholar**

---

Electrical and Computer Engineering Faculty  
Publications and Presentations

Electrical and Computer Engineering

---

10-2012

# Aspect-Dependent Radiated Noise Analysis of an Underway Autonomous Underwater Vehicle

John Gebbie  
*Portland State University*

Martin Siderius  
*Portland State University, siderius@pdx.edu*

John S. Allen III  
*University of Hawaii at Manoa*

Follow this and additional works at: [https://pdxscholar.library.pdx.edu/ece\\_fac](https://pdxscholar.library.pdx.edu/ece_fac)



Part of the [Electrical and Computer Engineering Commons](#)

**Let us know how access to this document benefits you.**

---

## Citation Details

Gebbie, J., Siderius, M., & Allen, J. (2012). Aspect-dependent radiated noise analysis of an underway autonomous underwater vehicle. *The Journal of The Acoustical Society of America*, 132(5), EL351-EL357.

This Article is brought to you for free and open access. It has been accepted for inclusion in Electrical and Computer Engineering Faculty Publications and Presentations by an authorized administrator of PDXScholar. Please contact us if we can make this document more accessible: [pdxscholar@pdx.edu](mailto:pdxscholar@pdx.edu).

# Aspect-dependent radiated noise analysis of an underway autonomous underwater vehicle

John Gebbie and Martin Siderius<sup>a)</sup>

*Northwest Electromagnetics and Acoustics Research Laboratory, Department of Electrical and Computer Engineering, Portland State University, 1900 SW 4th Avenue, Suite 160, Portland, Oregon 97201*  
jgebbie@ece.pdx.edu, siderius@pdx.edu

John S. Allen III

*Department of Mechanical Engineering, University of Hawai'i-Manoa, 2540 Dole Street, Holmes Hall 302, Honolulu, Hawaii 96822*  
alleniii@hawaii.edu

**Abstract:** This paper presents an analysis of the acoustic emissions emitted by an underway REMUS-100 autonomous underwater vehicle (AUV) that were obtained near Honolulu Harbor, HI using a fixed, bottom-mounted horizontal line array (HLA). Spectral analysis, beamforming, and cross-correlation facilitate identification of independent sources of noise originating from the AUV. Fusion of navigational records from the AUV with acoustic data from the HLA allows for an aspect-dependent presentation of calculated source levels of the strongest propulsion tone.

© 2012 Acoustical Society of America

**PACS numbers:** 43.30.Jx, 43.30.Zk, 43.30.Xm [AL]

**Date Received:** May 30, 2012     **Date Accepted:** September 3, 2012

## 1. Introduction

In the past several years, autonomous underwater vehicles (AUVs) have found a variety of uses in the commercial, military, and research sectors. Localization of surface craft have been investigated by a variety of methodologies such as shore-based radar, optical, thermal imaging, and more recently, acoustics.<sup>1</sup> However, AUVs pose a different detection challenge since no part of their hull extends above water and no surface wake is generated. Passive acoustic localization methods may be more practical than active methods in terms of cost and impact on the environment, but they require an accurate characterization of radiated noise from the target in terms of spectral content as well as aspect-dependent source levels. This paper aims to describe the azimuthal beam pattern of the strongest tone emitted from the propulsion system of an underway REMUS-100 AUV using a bottom-mounted horizontal line array (HLA).

Most AUVs are driven by electromagnetic propulsion systems, which can be the largest contributor of radiated noise. Several studies have been performed involving the collection of acoustic data generated from AUVs and analyzed the spectral content of their acoustic signatures.<sup>2-4</sup> Griffiths *et al.* (2001) analyzed the acoustic emissions of an Autosub AUV and found that it produced such low source levels that it was only detectable to within a few meters of their passive sonar equipment.<sup>4</sup> It was also hypothesized that propeller cavitation was the primary noise producer of this AUV since broadband emissions were detected up to roughly 4 kHz, with most acoustic energy concentrated in the lower band up to roughly 400 Hz. However, the Autosub may have been an anomalously quiet vehicle since other studies have since reported that higher source levels due to motor-borne vibrations found on some stock AUVs

---

<sup>a)</sup> Author to whom correspondence should be addressed.

could be reduced through mitigation strategies.<sup>3</sup> In contrast with broadband cavitation noise, these motor vibrations have narrow-band characteristics.<sup>3,5,6</sup> Radiation from wetted portions of an AUV's motor stator, and Helmholtz resonance of the fluid connection gap between the rotor and stator can lead to monopole radiation patterns, whereas alternating thrust (caused by non-sinusoidal motor currents, for example) can produce hull vibrations that radiate in a dipole manner.<sup>5</sup> Griffiths *et al.* (2001) reported their results as received levels, and noted that the levels appeared to increase sharply as the vehicle passed by the passive sonar equipment, which was likely due to a hull-masking effect.<sup>4</sup> The lack of ground truth measurements of the actual location of the AUV precluded calculation of source levels and beam patterns. Several studies have taken a more rigorous approach to measuring source levels and beam patterns by placing a REMUS-100 AUV in a bollard condition inside a tank.<sup>5-7</sup> However, there is limited published information on radiated noise characteristics of AUVs that are underway.

This study demonstrates a technique for characterizing the source levels and beam patterns of a REMUS-100 AUV in an underway condition by fusing navigational records from the AUV with acoustic data collected on a passive, bottom-mounted HLA. The AUV's navigational records serve multiple purposes in this analysis. A method for correcting small errors in the HLA's coordinates using cross-correlation of broadband modem noise is first developed. Navigational records are used to identify which signature components are originating from the AUV's propulsion system using beamforming. Using a basic characterization of the environment, propagation modeling tools produce an estimate of transmission loss (TL) between each position of the AUV and each hydrophone. Source levels are then computed with the passive sonar equation using the received level at each time step. The AUV's aspect with respect to the HLA is then derived from the AUV's position and heading at each time step, facilitating the calculation of the beam pattern.

## 2. Experiment

The AUV experiments were conducted in July 2010 at the Kilo Nalu Nearshore Reef Observatory (University of Hawai'i-Manoa) near Honolulu Harbor, Honolulu, HI. The observatory had several underwater electronics nodes, which supplied power and Ethernet connectivity to scientific equipment. One node was at a fixed site about 0.4 km from shore in 12 m of water. Honolulu Harbor was located 1 km to the northwest of this node, which served as a port for large commercial vessels. In addition, the nearby areas were popular sites for recreational fishing, boating, and scuba diving. There was also a significant amount of biological noise primarily from snapping shrimp, which created a loud, broadband clicking noise.

A hydrophone array (HTI-92-WB,  $-160$  dB re  $1$  V/ $\mu$ Pa) was connected to the node for a two-week period. The array was configured in a horizontal configuration, stretched out along the seafloor. This orientation provided azimuthal beam resolution facilitating direction-of-arrival (DOA) estimation of radiated noise from targets. It had a total of 23 elements evenly spaced at 0.5 m. The sample rate was 102.4 kHz with a dynamic range of 24 bits. The array used a high-pass filter to suppress frequencies below 300 Hz and a 110 dB anti-aliasing filter giving a usable acoustic band from 300 Hz to 46.4 kHz.

Acoustic data was collected on the array from a number of sources including a REMUS-100 AUV. The REMUS-100 was powered by a battery that can last up to 22 h, and driven by a direct-drive dc brushless motor, which turned an open three-blade propeller. It was 160 cm in length, 19 cm in diameter, and weighed 37 kg. It had a maximum water speed of 2.6 m/s and a maximum depth of 100 m. Onboard navigational sensors estimated its location via several methods. At the surface, satellite GPS was used to obtain a coordinate fix. An acoustic doppler current profiler was used to measure its velocity over the seabed after submerging. Long baseline navigation was also used, which involved acoustic interrogation of separately deployed transponders.

When both of these data streams were unavailable, the AUV defaulted to dead reckoning. Depth measurements were obtained from a pressure depth sensor. The AUV logged these navigational records in the form of downloadable, time stamped 3-D coordinates. An onboard acoustic modem, which operated in the 20–30 kHz band, was used to send data back to the operator in the boat. The modem served as a broadband source that proved useful for cross-correlation based DOA estimation.

In this experimental investigation, the AUV executed a pre-programmed mission. The AUV was deployed from a boat that motored a short distance away from the programmed AUV track. The boat engine was on for a few minutes and subsequently turned off. The modem transponder continued to transmit from the stationary boat. The AUV moved slowly at the surface for about 30 s before diving and accelerating to about 2.25 m/s. It followed a programmed track of several turns and course reversals passing the end of the array three times. On one turn, it reached a maximum distance of 100 m from the array. Figure 1(a) shows the path of the AUV relative to the array. The second plate shown in Fig. 1(b) will be discussed later. The AUV's acoustic modem broadcasted information to the boat every 30 s. Sample audio from the first and third passes are available in [Mm. 1](#) and [Mm. 2](#), respectively. These are provided for a qualitative sense of the noise emitted by the AUV in the presence of the competing background noise and interferers.

**Mm. 1.** Audio from the northernmost phone of the array as the AUV makes its first pass by the array. Background noise from the boat is audible (see spectrograms in Fig. 2). Snapping shrimp noise is also audible. Leakage of high-frequency modem noise into the human audible range is heard near the end of the segment. The sampling frequency of file is 44.1 kHz. This is a file of type “wav” (2.6 MB).

**Mm. 2.** Audio from the northernmost phone of the array as the AUV makes its first pass by the array. Background noise from the boat is audible (see spectrograms in Fig. 2). Snapping shrimp noise is also audible. Leakage of high-frequency modem noise into the human audible range is heard near the end of the segment. The sampling frequency of file is 44.1 kHz. This is a file of type “wav” (2.6 MB).

### 3. Methodology and results

Acoustic data from the northernmost element of the array during the first four minutes of the mission was used for the spectrograms shown in Fig. 2. In Fig. 2(a) the modem transmits data in the 20–30 kHz band in five second bursts every 30 s. Figure 2(b) illustrates various tones from the AUV propulsion system, which are visible upon

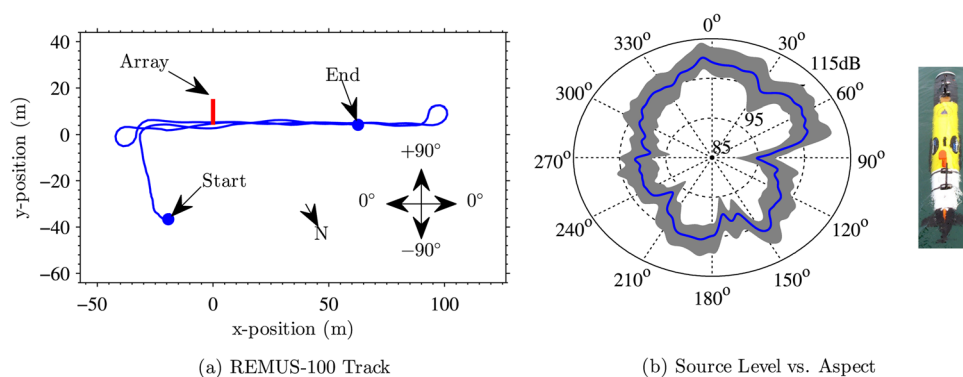


Fig. 1. (Color online) (a) Track of AUV showing its position relative to the array. Navigation records taken from the AUV were used to generate the track line. (b) AUV estimated source level (SL) as a function of aspect. The mean is represented by the dark line and the shaded region denotes the interquartile range. The front of the vehicle points towards zero degrees and is viewed top-down, as shown in the image on the right. Units are in dB re  $1 \mu\text{Pa}^2 / \text{Hz}$  at 1 m.

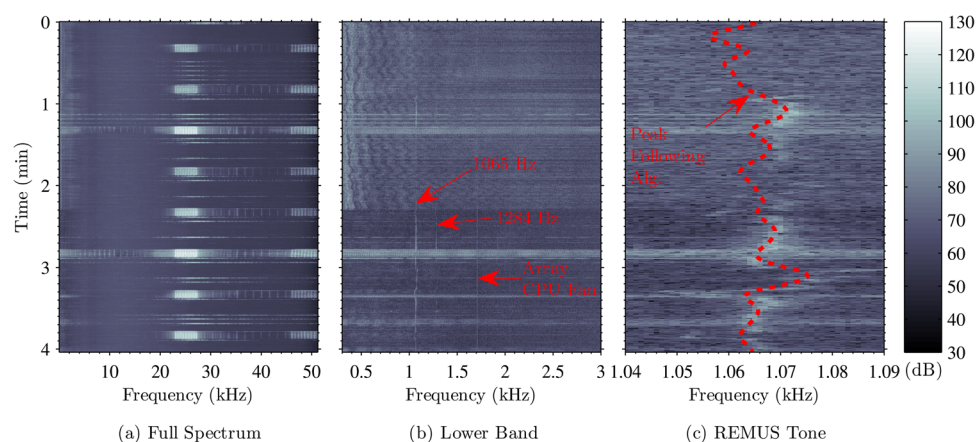


Fig. 2. (Color online) Spectrograms from the first phone of the array showing the signature of the REMUS-100 AUV and boat. Units are in dB re  $1 \mu\text{Pa}^2/\text{Hz}$ . (a) The full 300 Hz–51.2 kHz band in which the modem noise is visible. (b) Magnification of the 300 Hz–3 kHz band shows the various propulsion tones. (c) Magnification of the 1065 Hz propulsion tone showing the peak following algorithm (dashed line).

magnification of the frequency axis to 300 Hz–3 kHz. The strongest tone was centered at about 1065 Hz. Further magnification [Fig. 2(c)] reveals that this tone wandered within a 10 Hz band. The tone faded toward the end of the first minute and again at the beginning of the third minute. This corresponds to times during which the AUV turned  $180^\circ$ . The gap at the beginning of the dataset was most likely due to the AUV slowly moving at the surface. The 1700 Hz tone originated from a CPU fan inside the array electronics pressure vessel. The source level of the modem was sufficiently high that when within a few meters of the array it overcame the 110 dB anti-aliasing filter in the array and leaked energy into the lower frequency bands. This is most apparent at the time offsets of 1.3, 2.7, 3.2, and 3.5 minutes.

The broadband modem noise was the highest SNR signal emanating from the AUV, as seen in Fig. 2(a). This was used, along with the propagation delay of sound in water, to estimate the direction of the signal relative to the orientation of the array. With two hydrophones, the time-of-arrival difference was easily measured by cross-correlating their signals. The phones at opposite ends of the array were selected due to their farthest separation distance. Cross-correlating time series data from each phone produced another time series in which the time-axis corresponded to time-of-arrival differences. For a sufficiently coherent broadband signal, such as that of the modem, a peak appeared at an offset corresponding to the delay of that signal between the two hydrophones. This was computed in the frequency domain with a pre-whitening filter. Pre-whitening preserves the phase information while forcing the power spectrum to be white. This technique improves results for source signals which are not initially spectrally white.

Each peak in the cross-correlation output produced an isodiachron, a hyperboloid surface in 3-D space (assuming an isospeed), corresponding to all possible target locations having the same time-of-arrival differences. In the far field, this was approximated using the asymptotes of the hyperboloid, which trace out a cone. In 2-D, this reduced to a DOA with the angle measured from the broadside and originating from the center of the array.

Figure 3(a) shows a bearing-time-record (BTR) plot in which the cross-correlation time series was converted to DOA angles and plotted along the horizontal axis. The data was divided into short time windows, and DOA angles from each are plotted on the vertical axis. The dashed line shows the DOA angle based on navigational records downloaded from the AUV after the mission. The boat track is visible



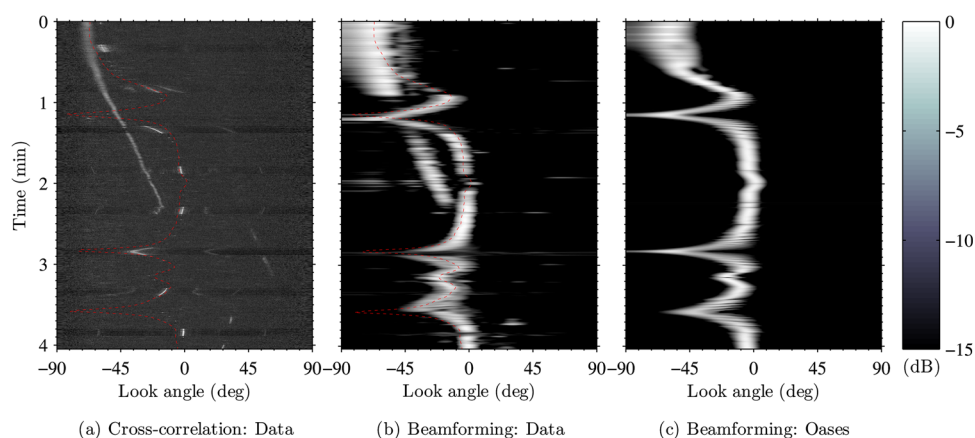


Fig. 3. (Color online) Bearing-time-record (BTR) plots. Dashed lines are DOA angles computed from navigational records downloaded from the AUV. (a) Two-hydrophone cross-correlation algorithm. The boat track is visible during the first few minutes. The AUV's modem produces a very strong peak every 30 s. (b) Conventional narrowband beamforming applied to acoustic data recorded on the array at around 1065 Hz. (c) Same algorithm using simulated data at 1065 Hz created with navigational records from the AUV using OASES.

during the first two minutes but disappeared after its engine was shut off. Strong peaks in the BTR correspond to the modem, but vanish during the time intervals when the modem is not transmitting. A good agreement exists between the navigational records and the cross-correlation analysis during the “on” periods and for sufficient angular separation from the nearby boat.

A genetic algorithm was used to find the “best set” of coordinates and orientation for the array, where “best set” is defined by that which minimizes an objective function computed as the sum square difference between each set of DOA angles over the entire four minute dataset. The optimum array location was about 7.6 m northwest from its initial estimated location, and its orientation rotated about  $4^\circ$  counterclockwise. This was a reasonable amount of correction based on the amount of navigational precision used during deployment.

In Fig. 2(b), several tones can be attributed to the propulsion noise with the strongest centered about 1065 Hz. Given the extremely narrowband nature of this source, a conventional (delay-and-sum) beamformer computed in the frequency domain at the bin corresponding to this specific frequency tracked the DOA angle accurately, as shown in Fig. 3(b). A Hann window was applied to individual, overlapping snapshots in the time domain during averaging, and a Taylor window was multiplied to the steering vector for additional side lobe suppression (i.e., array shading). The maximum achievable gain (in terms of signal power) for an unshaded conventional beamformer on a  $N$  element array is  $10 \log_{10}\{N/[1 + (n-1)\rho]\}$ , where  $\rho$  is the correlation coefficient of noise.<sup>8</sup> For this 23-element array, the array gain was 11.7 dB, with a standard deviation of 2.6 dB, and a  $\rho$  of 0.04. Decibels for array gain and  $\rho$  are both in reference to unit-less quantities.

The cross-correlation BTR in Fig. 3(a) localizes targets having broadband signatures, whereas the beamforming BTR in Fig. 3(b) is specific to targets producing energy in a very narrow band. However, broadband sources that overlap the narrow band gap were also detected by the beamformer. Hence the boat track, which produced broadband energy from a few Hz to roughly 6 kHz, appears in both the cross-correlation BTR as well as the beamforming BTR ( $\sim 1065$  Hz). Notably, a continuous track for the AUV is visible using beamforming [Fig. 3(b)], but only appears in limited segments using cross-correlation [Fig. 3(b)].

One challenge of this AUV was the wandering nature of the tones seen in Fig. 2(c). A simple peak following algorithm was created in an attempt to keep the

beamformer locked onto the strongest tone. In each row of the spectrogram, the tallest peak was chosen inside of a narrow band centered at 1065 Hz. These data were smoothed using a low pass filter to obtain the curve shown in Fig. 2(c). It was expected that improvement from peak following could be more substantial for data collected over a longer period of time. At the end of the four-hour AUV mission the 1065 Hz tone had drifted to about 1000 Hz, possibly caused by a lower current draw from the battery.

For further verification of the AUV track [Fig. 3(b)], the AUV's navigational records were passed into the OASES software for simulated snapshots of data at every position. OASES is a full-wave propagation model based on a numerical wavenumber integration solution to the acoustic wave equation.<sup>9</sup> The simulation was configured with a pressure release surface, flat half-space seabed, and isovelocity water with parameters  $c = 1500$  m/s. The seabed parameters, based on a composition of medium/coarse sand that were consistent with grab samples taken at the deployment site, were  $c = 1836$  m/s,  $\alpha = 0.88$  dB/ $\lambda$ , and  $\rho = 2.151$  g/cm<sup>3</sup>.<sup>10</sup> The results of this simulated data using the same beamformer are shown in Fig. 3(c). There is excellent agreement between the experimental data and the simulated results indicating that the 1065 Hz tone was indeed emitted by the AUV.

Source level (SL) measurements of the AUV's propulsive emissions were computed by adding the received level (RL) to an estimate of the transmission loss (TL). OASES was used to estimate TL between the AUV source and different elements of the array. The AUV's heading was computed by taking the time-derivative of the AUV's position vector. Ocean currents measured by the observatory were on the order of 2–3 cm/s, so deviation between the AUV's heading and course were negligible. Combining the AUV position and heading with coordinate estimates of array elements allowed the AUV's aspect relative to each element to be computed. For this study, a subarray of eight equally spaced elements from the array were selected and the SL was computed as a function of aspect independently for each element. Since the 1065 Hz tone disappeared when the AUV maneuvered, this had the potential to bias the SL estimate. To avoid this, only time segments corresponding to constant speed, heading, and depth of the AUV were considered. The SL of the propulsive tone as a function of aspect is shown in Fig. 1(b). The dark line represents the mean, and the shaded region denotes the interquartile range. Using multiple elements spread out over the entire array allowed for greater aspect coverage than would have for a single element. An additional 37 minutes of acoustic data was added to this part of the analysis, which included additional AUV passes by the HLA. The mean SL normalized over the full 360° aspect range for the 1065 Hz propulsion tone was 104.8 dB re 1  $\mu$ Pa<sup>2</sup>/Hz at 1 m, with a standard deviation of 8.4 dB re 1  $\mu$ Pa<sup>2</sup>/Hz at 1 m. The levels reported here are slightly lower than, but consistent with, the values measured using tank experiments reported by Holmes *et al.*<sup>5,6</sup> Ambient noise RL was measured at 60.9 dB re 1  $\mu$ Pa<sup>2</sup>/Hz, with a standard deviation of 6.0 dB re 1  $\mu$ Pa<sup>2</sup>/Hz. When the AUV was between 10 and 50 m from the hydrophones, the mean signal to interference plus noise ratio was 19.4 dB with a standard deviation of 7.6 dB. All decibel calculations were consistent with the methods used by Ainslie.<sup>10</sup> Variations of SLs between snapshots were partly attributed to mismatch between actual and modeled environmental parameters. Additionally, localized obstructions, such as coral reefs extending a few meters above the seabed in some areas, might have impeded propagation. Unmodeled factors such as bathymetric variations and surface scattering might also have contributed to the observed variability.

#### 4. Conclusion

This paper quantifies, for the first time, the acoustic source levels and beam pattern of the strongest propulsion-system-borne tone emitted from an underway REMUS-100 AUV by fusing acoustic data from a fixed HLA with the AUV's navigation records. The directionality of the tone and the broadband modem signal with respect to the

HLA were consistent with the navigational records, thus validating that these signals were indeed emitted by the AUV. Propagation analysis was performed using OASES in which the time-varying TL was calculated between the maneuvering AUV and the array. A complementary simulation of the radiated tone was also performed with OASES enabling discrimination between the AUV target and a boat interferer.

Further studies might include incorporation of bathymetric information into propagation models. Less prominent tones could also be analyzed for aspect-dependence. Since AUV maneuvering resulted in a change in frequency, or a diminished primary propulsion tone, a further study might investigate beam patterns for a maneuvering target.

### Acknowledgments

The authors acknowledge support for this research by the Office of Naval Research for the development of the beamforming and propagation methodology, as well as the fellowship of J.G. We thank the Department of Homeland Security for sponsoring J.S.A., and for the experimental deployment under Grant Award No. 2008-ST-061-ML0001. We also thank Portland State University for funding. Additionally, we thank the Kilo Nalu Nearshore Reef Observatory, and Tom Monroe of High Tech, Inc. for technical support.

### References and links

- <sup>1</sup>K. W. Chung, A. Sutin, A. Sedunov, and M. Bruno, "DEMON acoustic ship signature measurements in an urban harbor," *Adv. Acoust. Vib.* **2011**, 1–13 (2011).
- <sup>2</sup>W. M. Carey, J. D. Holmes, and J. F. Lynch, "The applicability of a small autonomous vehicle towed array system to ocean acoustic measurements and signal processing," *Proc. Meet. Acoust.* **4**, 070007 (2009).
- <sup>3</sup>R. Zimmerman, G. L. D'Spain, and C. D. Chadwell, "Decreasing the radiated acoustic and vibration noise of a mid-size AUV," *IEEE J. Ocean. Eng.* **30**, 179–187 (2005).
- <sup>4</sup>G. Griffiths, P. Enoch, and N. W. Millard, "On the radiated noise of the autosub autonomous underwater vehicle," *ICES J. Mar. Sci.* **58**, 1195–1200 (2001).
- <sup>5</sup>J. D. Holmes, W. M. Carey, and J. F. Lynch, "An overview of unmanned underwater vehicle noise in the low to mid frequencies bands," in *POMA—159th Meeting Acoustical Society of America/NOISE-CON 2010* (2010), p. 065007.
- <sup>6</sup>J. D. Holmes, "Investigation of ocean acoustics using autonomous instrumentation to quantify the water-sediment boundary properties," Ph.D. thesis, Boston University College of Engineering, Boston, MA, 2007.
- <sup>7</sup>J. D. Holmes, W. M. Carey, J. F. Lynch, A. E. Newhall, and A. Kukulya, "An autonomous underwater vehicle towed array for ocean acoustic measurements and inversions," in *Oceans 2005—Europe*, IEEE (2005), Vol. 2, pp. 1058–1061.
- <sup>8</sup>R. J. Urick, *Principals of Underwater Sound for Engineers* (McGraw-Hill, New York, 1967).
- <sup>9</sup>H. Schmidt, *OASES User Guide and Reference Manual*, Department of Ocean Engineering at Massachusetts Institute of Technology, Cambridge, MA, <http://oceanai.mit.edu/lamss/pmwiki/pmwiki.php?n=Site.Oases>, 3.1 ed. (last viewed March 11, 2011).
- <sup>10</sup>M. A. Ainslie, *Principles of Sonar Performance Modelling (Springer Praxis Books/Geophysical Sciences)*, 1st ed. (Springer-Verlag, Berlin, 2010).